CDF note 7907

Study of $B_s^0 \to D_s^- \ell^+ X$ Oscillations in the Two-Track Trigger Data Sample

The CDF Collaboration
URL http://www-cdf.fnal.gov

(Dated: October 24, 2005)

We search for B_s^0 flavor oscillations using $B_s^0 \to D_s^- \ell^+ X$ decays recorded with the CDF II Detector during the Run II data taking period of the Fermilab Tevatron Collider. The D_s^- mesons are reconstructed in three decay modes: $D_s^- \to \phi\pi^-$, $D_s^- \to K^{*0}K^-$ and $D_s^- \to \pi^+\pi^-\pi^-$. Opposite side lepton and jet charge flavor taggers provide information about the b-quark flavor at the time of production of the B_s^0 meson. Using an amplitude scan method, we obtain

$$\begin{aligned} \Delta m_s &> 6.7\ \mathrm{ps}^{-1} \text{ @ } 95\% \text{ C.L.} \\ \text{expected sensitivity} &= 10.4\ \mathrm{ps}^{-1} \end{aligned}$$

Preliminary Results for PANIC05, October 24-28 2005

I. INTRODUCTION

In the Standard Model, the B_s^0 meson exists in two CP-conjugate states, $|B_s^0\rangle = |\bar{b}s\rangle$ and $|\bar{B}_s^0\rangle = |b\bar{s}\rangle$. The 'heavy' and 'light' mass eigenstates of the B_s^0 meson, B_s^H and B_s^L, are mixtures of the two CP-conjugate states. The probability for a B_s^0 meson produced at proper time $t = 0$ to decay as $\bar{B}_s^0$ at proper time $t > 0$ is given by

$$\mathcal{P}(B_s^0 \to \bar{B}_s^0) \;=\; \frac{1}{2\tau_s} e^{-\frac{t}{\tau_s}} \left[1 - \cos\left(\Delta m_s\, t\right)\right] \tag{1}$$

where CP violation, as well as a possible lifetime difference between the heavy and light mass eigenstates of the B_s^0 meson, have been neglected, and $\Delta m_s \equiv m_H - m_L$ is the oscillation frequency. The 95% C.L. limit for the mass difference is $\Delta m_s > 14.4$ ps^{-1} [1]. In this analysis we search for B_s^0 flavor oscillations using $B_s^0 \to D_s^- \ell^+ X$ decays, recorded with the CDF II Detector [2] during the Run II data taking period of the Fermilab Tevatron Collider.

II. DATA SAMPLE & EVENT SELECTION

This analysis is based on an integrated luminosity of ~ 355 pb^{-1}, collected by the CDF II Detector between March 2002 and August 2004. The data is gathered with the so-called "Two-Track Trigger" (TTT), which selects events that contain track pairs with transverse momentum larger than 2 GeV/c and 120 μm $< d_0 <$ 1 mm, with d_0 the impact parameter of a track. These tracks are referred to as "SVT tracks". Three B_s^0 meson final states are reconstructed in this analysis (references to a specific charge state imply the charge-conjugate state as well):

$$\begin{aligned}
B_s^0 &\to D_s^- \ell^+ X, \quad D_s^- \to \phi\pi^-, \quad \phi \to K^+K^-; \\
B_s^0 &\to D_s^- \ell^+ X, \quad D_s^- \to K^{*0}K^-, \quad K^{*0} \to K^+\pi^-; \\
B_s^0 &\to D_s^- \ell^+ X, \quad D_s^- \to \pi^+\pi^-\pi^-.
\end{aligned}$$

A similar analysis has been performed in the "lepton + displaced track" (ℓ+SVT) trigger data sample [3]. By moving on to the TTT sample we gain significantly in statistics, by lowering the transverse momentum requirement of the lepton from 4 GeV/c in the ℓ+SVT trigger to 1.5 GeV/c in the TTT. About 60% of the events used in the former analysis are part of the current one, and therefore the results are correlated. The improvements besides the increase in statistics are the following: the $\ell^+ D_s^-$ invariant mass is on average significantly lower for background events than for real B_s^0 signal events. This variable has been found to be extremely important, as the level of background in the TTT sample is significantly higher than in the ℓ+SVT sample. For the flavor tagging, a new version of the Jet Charge Tagger based on a Neural Network has been applied [4]. Finally, additional hits in the innermost silicon layer are added to the tracks after the standard track reconstruction, and an event-by-event primary vertex is used instead of an average beam position.

The reconstruction of the $B_s^0 \to D_s^- \ell^+ X$ signal starts by forming the D_s^- candidates. The daughter tracks of the D_s^- candidate are fit with a common vertex constraint. In the next step, the B_s^0 vertex is found from the intersection of the lepton trajectory and the flight path of the D_s^- meson. In those cases where the lepton is a SVT track, the candidate is called "lepton SVT". Otherwise both SVT tracks will belong to the D_s^- meson, and the candidate is known as "lepton non-SVT". The effect of the Two-Track Trigger is different in these two groups of candidates, and therefore they are treated separately in this analysis. The selection cuts are summarized in Table I. In that table, the vertex probability $\mathcal{P}(B_{vertex})$ and the vertex χ^2_{xy} are given by three– and two– dimensional vertex fits, respectively. The quantity L_{xy} stands for the decay length on the transverse plane.

One of the cuts that appear in Table I corresponds to the helicity angle ψ. Such angle is calculated in the ϕ or K^{*0} rest frame, and it is defined as the angle between the momentum of the D_s^- candidate and the direction of the two decay products, e.g., $\phi \to K^+K^-$. In Table I we are not including those cuts that are common to the three decay modes, summarized here:

$D_s^- \to \phi\pi^-$	$D_s^- \to K^{*0}K^-$	$D_s^- \to \pi^+\pi^-\pi^-$
$\mathcal{P}(B_{vertex}) > 10^{-7}$	$\mathcal{P}(B_{vertex}) > 10^{-5}$	$\mathcal{P}(B_{vertex}) > 10^{-5}$
$\chi^2_{xy}(D_s^-) < 20$	$\chi^2_{xy}(D_s^-) < 20$	$\chi^2_{xy}(D_s^-) < 20$
$L_{xy}/\sigma_{L_{xy}}(D_s^- \to PV) > 5$	$L_{xy}/\sigma_{L_{xy}}(D_s^- \to PV) > 8$	$L_{xy}/\sigma_{L_{xy}}(D_s^- \to PV) > 11$
—	$L_{xy}/\sigma_{L_{xy}}(B_s^0 \to PV) > 2$	$L_{xy}/\sigma_{L_{xy}}(B_s^0 \to PV) > 2$
$\lvert cos\,\psi\rvert > 0.3$	$\lvert cos\,\psi\rvert > 0.3$	—
$p_T(K^\pm) > 0.7$ GeV/c	$p_T(K^\pm, \pi^-) > 0.7$ GeV/c	$p_T(\pi^\pm) > 0.7$ GeV/c
$\lvert M_\phi^{PDG} - m_{K^+K^-}\rvert < 12$ MeV/c^2	$\lvert M_{K^{*0}}^{PDG} - m_{K^+\pi^-}\rvert < 60$ MeV/c^2	—

TABLE I: Selection criteria.

- $-0.01 < L_{xy}(D_s^- \to B_s^0)\frac{m_{D_s^-}}{p_T(D_s^-)} < 0.10$ cm;
- $2.9 < m_{\ell^+ D_s^-} < 5.3$ GeV/c^2;
- $\sigma_{ct^*}(B_s^0) < 0.04$ cm;
- $ct^* > 0.01$ cm ($ct^* > 0.005$ cm for the $\phi\pi^-$ lepton SVT candidates).

To identify the lepton tracks we use particle identification likelihoods, $\mathcal{L}_\ell$, that were originally developed for the opposite side soft lepton taggers [5]. In addition to the sample splitting mentioned before, we further divide it depending if the lepton is a muon or an electron. To select muons, we cut at different values of the particle identification likelihood, depending on the muon detector, whereas for electrons a common cut is applied. Due to the incomplete reconstruction of the B_s^0 decays, it is not possible to fully reconstruct the B_s^0 mass. Instead the D_s^- mass distributions are used to to compute the yield for each channel, shown in Table II.

physics background	$\frac{S}{B}$	$\frac{S}{\sqrt{S+B}}$	S
$\mu^+ D_s^-$, $D_s^- \to \phi\pi^-$	3.0	68	6,250 ± 110
$\mu^+ D_s^-$, $D_s^- \to K^{*0}K^-$	0.7	31	2,387 ± 87
$\mu^+ D_s^-$, $D_s^- \to \pi^+\pi^-\pi^-$	0.3	22	2,208 ± 142
$e^+ D_s^-$, $D_s^- \to \phi\pi^-$	2.8	51	3,565 ± 85
$e^+ D_s^-$, $D_s^- \to K^{*0}K^-$	0.6	22	1,307 ± 67
$e^+ D_s^-$, $D_s^- \to \pi^+\pi^-\pi^-$	0.4	17	1,167 ± 80

TABLE II: Signal over background ratio $\frac{S}{B}$, $\frac{S}{\sqrt{S+B}}$ and number of signal candidates S.

A. Physics Backgrounds

These are real physics processes with the correct charge correlation between the lepton and the D_s^- meson, feeding into our decay signatures. For every physics background, a Monte Carlo sample has been produced to compute their fractions in the signal region, summarized in Table III. The $B_s^0 \to D_s^{(*)} D^{(*)} X$ background is almost completely removed, mainly due to the $m_{\ell^+ D_s^-}$ cut. The backgrounds with non-negligible contribution will be treated like signal, i.e., they will have associated specific ct^*-efficiencies and k-factor distributions.

B. Prompt Background

This background consists of two components: a real D_s^- meson and a fake lepton; and a real D_s^- meson and a real lepton from a $c\bar{c}$ event. The fraction of prompt background from $c\bar{c}$ events is very

decay	f_{phys} [%] $\phi\pi^-$	$K^{*0}K^-$	$\pi^+\pi^-\pi^-$
$B_s^0 \to D_s^{(*+)} D_s^{(*-)} X,\ D_s^{(*)} \to \mu^+ Y$	3.0 ± 0.9	3.0 ± 0.9	2.9 ± 0.9
$B_u^+ \to D_s^{(*)} D^{(*)} X,\ \ D^{(*)} \to \mu^+ Y$	6.2 ± 2.5	6.2 ± 2.5	6.0 ± 2.4
$B_d^0 \to D_s^{(*)} D^{(*)} X,\ \ D^{(*)} \to \mu^+ Y$	6.3 ± 2.5	6.3 ± 2.5	6.0 ± 2.4
$B_s^0 \to D_s^{(*+)} D_s^{(*-)} X,\ D_s^{(*)} \to e^+ Y$	2.1 ± 0.6	2.3 ± 0.7	1.7 ± 0.5
$B_u^+ \to D_s^{(*)} D^{(*)} X,\ \ D^{(*)} \to e^+ Y$	5.4 ± 2.2	5.1 ± 2.0	5.2 ± 2.1
$B_d^0 \to D_s^{(*)} D^{(*)} X,\ \ D^{(*)} \to e^+ Y$	5.3 ± 2.1	5.0 ± 2.0	5.1 ± 2.0

TABLE III: Expected fraction of each physics background with respect to the signal + physics backgrounds.

small, mainly thanks to the cuts on ct^*. To obtain a sample of fake leptons and real D_s^- mesons, we apply a lepton identification likelihood cut of $\mathcal{L}_\ell \leq 0.05$; we assume that the ct^* distribution of the prompt background coming from $c\bar{c}$ events has the same shape as the ct^* distribution from fake leptons. The fraction of prompt background is determined from fits to the $m_{\ell^+ D_s^-}$ invariant mass distribution. We can see some $m_{\ell^+ D_s^-}$ invariant mass distributions in Figure 1.

III. MASS & LIFETIME ANALYSIS

Mass and lifetime fits are mandatory steps when performing a B mixing analysis. Both mass and lifetime distributions are determined from an unbinned maximum likelihood fit to the D_s^- meson mass and the pseudo proper decay-length of the B_s^0 meson, ct^*, defined in Equation 2.

$$ct(B_s^0) \equiv ct^*\, k; \qquad ct^* \equiv M_{B_s^0}^{PDG} \frac{L_{xy}(\ell^+ D_s^-)}{p_T(\ell^+ D_s^-)}; \qquad k \equiv \left\langle \frac{p_T(\ell^+ D_s^-)}{p_T(B_s^0)} \frac{L_{xy}(B_s^0)}{L_{xy}(\ell^+ D_s^-)} \right\rangle_{\rm MC} \tag{2}$$

The proper decay-length ct of the B_s^0 candidates is determined from measured quantities of the $\ell^+ D_s^-$ pair and Monte Carlo-derived average corrections, i.e., k-factor distributions, to account for missing particles. These k-factor distributions can be seen in Figure 2. The overall likelihood $\mathcal{L}$ consists of terms describing the signal and background (combinatorial, prompt and physics) probabilities,

$$\mathcal{L} = f_{signal}\, \mathcal{L}_{signal} + f_{comb}\, \mathcal{L}_{comb} + f_{prompt}\, \mathcal{L}_{prompt} + f_{phys}\, \mathcal{L}_{phys}\, ; \qquad \mathcal{L}_i = \mathcal{L}_i^m\, \mathcal{L}_i^{ct^*}\, \mathcal{L}_i^{\sigma_{ct^*}} \tag{3}$$

where f_i are the fractions of the different contributions in the likelihood. In Equation 3 we can see that each contribution $\mathcal{L}_i$ is formed as the product of normalized probability terms describing the D_s^- mass, the pseudo proper decay-length ct^* and the pseudo proper decay-length error σ_{ct^*}. The latter, $\mathcal{L}_i^{\sigma_{ct^*}}$, is simply a normalized histogram which has been obtained by filling in the values of σ_{ct^*} from the data samples.

The signal, prompt and physics backgrounds mass components are well described by a common double gaussian, while the combinatorial background is accurately described with a first order polynomial term. The signal ct^* term is composed of an exponential decay which is convoluted with a gaussian resolution function. This is smeared with the normalized k-factor distribution $F(k)$, and finally multiplied by the ct^*-efficiency function $\xi(ct^*)$. This efficiency curve is extracted from Monte Carlo simulation, and it is needed in order to describe the effect of trigger and selection cuts on the exponential lifetime (different efficiency curves can be seen in Figure 3).

$$\mathcal{L}_{signal}^{ct^*} = \frac{k}{c\tau} \exp\left(-\frac{k\, ct^{*\prime}}{c\tau}\right) \otimes G(ct^* - ct^{*\prime}; S_{ct^*}\sigma_{ct^*}) \otimes F(k)\, \xi(ct^*) \tag{4}$$

where S_{ct^*} is the overall scale factor for the assumed gaussian resolution. The combinatorial background ct^* shape is extracted from the D_s^- mass sidebands, and it is empirically modelled. The ct^* distributions of the prompt background have also been empirically described. As we mentioned before, the physics backgrounds are described with expressions equivalent to that of the signal

The fit results projected over the mass and the pseudo proper decay-length distributions can be found in Figures 4-7. All parameters used in the description of the pseudo proper decay-length distributions are fixed in the following fits, and the B lifetimes are fixed to their PDG values.

IV. AMPLITUDE ANALYSIS

The general likelihood definition of Equation 3 remains valid here if we add an extra multiplicative factor $\mathcal{L}_i^D$. This new term represents the flavor tagging dilution PDF, and it is described by normalized histograms. The search for B_s^0 oscillations is based on an amplitude scan [7] over values of the Δm_s oscillation frequency. The amplitude parameter A enters in the ct^* signal likelihood of tagged candidates,

$$\mathcal{L}_{signal}^{ct^*} = \begin{cases} (1-\sum_i \epsilon_i)\,\frac{k}{c\tau}\,e^{-\frac{k\,ct^{*\prime}}{c\tau}} \otimes \mathcal{G} \otimes F(k) & \forall\ tag^i = 0 \\ \frac{\epsilon_i}{2}\left[1 \pm A\,S_D^i\,D\,\cos(\Delta m_s\,k\,ct^{*\prime})\,\frac{k}{c\tau}\,e^{-\frac{k\,ct^{*\prime}}{c\tau}}\right] \otimes \mathcal{G} \otimes F(k) & \text{for } tag^i = \pm 1 \end{cases} \tag{5}$$

$$\mathcal{G} \equiv G(ct^* - ct^{*\prime}; S_{ct^*}\sigma_{ct^*})\,\xi(ct^*)$$

where ϵ_i is the efficiency of the flavor tagger i, D is the event dilution and S_D^i is the dilution scale factor of the flavor tagger i, determined in [8]. For the combinatorial background a potential global tagging asymmetry is allowed.

A. Flavor Taggers

Three opposite side flavor taggers are used in this analysis: Soft Muon Tagger (SMT), Soft Electron Tagger (SET) [5] and Jet Charge Tagger. An improved version of the Jet Charge Tagger with respect to the Winter 2005 results [3] is applied, based on Neural Networks [4]. The Jet Charge Tagger is divided in three categories, based on the tagging jet type: jets that contain a secondary vertex (JVX); jets with displaced tracks but no secondary vertex (JJP); and the highest P_T jet in the event with neither a displaced vertex nor displaced tracks (JPT).

For a B_s^0 meson candidate we may have several tags of the production b-flavor, provided by several taggers. To choose a decision among them, the taggers are arranged hierarchically in order of average dilution. Following this exclusive hierarchy, the tagger decisions are kept uncorrelated. Then, we check whether the best tagger has provided a decision. If that is not available we move to the second best and so on.

B. Amplitude Scan

We perform an amplitude scan, where we fit for the amplitude at different potential Δm_s values. In the case of infinite statistics, perfect ct resolution and perfect tagger parameterization and calibration, one would expect A to be unit for the true oscillation frequency and zero for the remaining of the probed spectrum. In practice, the output is a list of values $\{A,\ \sigma_A^{stat}\}(\Delta m_s)$.

Our aim is to estimate the largest Δm_s value up to which we can exclude all mixing frequencies at 95% confidence level. This corresponds to the smallest value of Δm_s where $A + 1.645\,\sigma_A = 1$. The expected sensitivity is defined as the value of Δm_s for which $1.645\,\sigma_A = 1$. The predicted significance $\mathcal{S}$ has the following expression,

$$\mathcal{S}(\Delta m_s) \ \equiv\ \frac{A}{\sigma_A} = \frac{S}{\sqrt{S+B}}\sqrt{\frac{\epsilon\mathcal{D}^2}{2}}\exp\left(-\frac{1}{2}\sigma_{ct}^2\Delta m_s^2\right) \tag{6}$$

where S is the number of signal events, B is the number of background events, $\epsilon\mathcal{D}^2$ is the tagging performance and σ_{ct} is the ct resolution. The decays used in this analysis are partially reconstructed, and therefore the ct resolution suffers from the uncertainty in L_{xy} and the simulation k factor smearing.

V. SYSTEMATIC UNCERTAINTIES

The discussion in Reference [7] details the prescription for setting a limit on Δm_s within an amplitude scan. The systematic uncertainty of the amplitude is

$$\sigma_A^{syst} \;=\; \Delta A + (1 - A)\,\frac{\Delta\sigma_A^{stat}}{\sigma_A^{stat}} \tag{7}$$

where ΔA and $\Delta\sigma_A^{stat}$ are the changes in the amplitude and its statistical error induced by a particular systematic effect. In this analysis, large ensembles of toy Monte Carlo experiments are used to evaluate the systematic uncertainty on the amplitude scan at several Δm_s points. Two sets of toy Monte Carlo are needed, having one of them with the default settings and the other one with the systematic effect shifted. An amplitude scan is then performed for each set of toy Monte Carlo configuration, and the resulting systematic uncertainty is defined by the mean of the errors according to Equation 7. The following sources of systematic uncertainties have been studied:

a. Monte Carlo lifetime in ct^*-efficiency curve. The shape of this curve depends on the B_s^0 lifetime assumed in Monte Carlo. We vary the Monte Carlo lifetime within the PDG errors.

b. Physics backgrounds. These have large uncertainties in their branching ratios. The associated uncertainty is determined by shifting $\pm\sigma$ their fractions.

c. $c\tau(B_s^0)$ fixed to the PDG value. We vary the lifetime within the PDG errors.

d. Scale factor on σ_{ct^*}. One of the model parameters is the scale factor for the error on the decay vertex position. This scale factor is determined in [6], and we vary it according to the uncertainties quoted there.

e. Background parameterization from the sidebands. The combinatorial background parameterization is computed using the D_s^- mass sidebands. We shift the sidebands windows ± 50 MeV/c from the nominal values.

f. Dilution scale factors. The uncertainties on the amplitude related to the dilution scale factors are evaluated by modifying them in the fit taking into account the errors on the calibrated values [8].

g. Prompt background. There are two uncertainties related to the prompt background, its ct^* shape and its fraction. We vary the shape within the uncertainties we got from the fit to the fake lepton sample. The fraction of the prompt background has been obtained from a fit to the $m_{\ell^+ D_s^-}$ distribution, and we use the uncertainty of this fit to study the related systematic. In the final fit, the dilution of the prompt background is fixed to zero. For the study of systematic uncertainties, we varied the dilution within $\pm$ the value obtained for the signal.

h. Possible high value of $\Delta\Gamma/\Gamma$. If the value of $\Delta\Gamma/\Gamma$ is high, the PDF for the signal in the ct^* space can not be described as a simple exponential modulated by a fast oscillating term. We study the effect of having a non-zero width difference between the heavy and light B_s^0 states using a toy Monte Carlo approach. We use a conservative value of $\Delta\Gamma/\Gamma = 0.2$.

i. Non-gaussian detector resolution. The nominal fit model assumes the detector resolution to be perfectly gaussian, with the width of the spread equal to the ct^* error scaled by S_{ct^*}. As a systematic study we have added an additional gaussian plus an exponential tails, regarding the results in [6].

The systematic uncertainties are then combined by adding them in quadrature for a given Δm_s value. The 95% C.L. exclusion limit is finally obtained as

$$A \;+\; 1.645\sqrt{\sigma_A^{stat}(\Delta m_s)^2 + \sigma_A^{syst}(\Delta m_s)^2} < 1 \tag{8}$$

The evaluated systematic uncertainties are summarized in Table IV. Finally, these values are interpolated for all other Δm_s points in the scan, as can be seen in Figure 8. The amplitude scan with statistical and systematic uncertainties is shown in Figure 9.

source of systematics	$\sigma_A^{syst}(\Delta m_s)$ @ Δm_s 0 ps^{-1}	5 ps^{-1}	10 ps^{-1}	15 ps^{-1}	20 ps^{-1}
$c\tau$ in MC	0.0005	0.0007	0.0010	0.0013	0.0017
SVT parameterization	0.0007	0.0007	0.0009	0.0010	0.0013
physics backgrounds	0.1066	0.0410	0.0442	0.0536	0.0602
$c\tau(B_s^0)$	0.0011	0.0060	0.0147	0.0206	0.0351
S_{ct^*}	0.0007	0.0189	0.0236	0.0303	0.0698
combinatorial background	0.0111	0.0210	0.0294	0.0362	0.0423
dilution scale factors	0.0472	0.0543	0.0544	0.0613	0.0725
sample composition	0.0021	0.0037	0.0054	0.0063	0.0098
prompt background dilution	0.0357	0.0266	0.0572	0.0746	0.1091
prompt background fraction	0.0123	0.0235	0.0402	0.0947	0.1668
prompt background ct^* shape	0.0013	0.0053	0.0128	0.0391	0.0601
$\Delta\Gamma/\Gamma$	0.0010	0.0285	0.0305	0.0289	0.0287
non-gaussian tail	0.0063	0.0319	0.0796	0.0938	0.1254
total systematic	0.1232	0.0927	0.1375	0.1871	0.2771
statistical	0.0878	0.2523	0.5645	0.7581	2.8501

TABLE IV: Summary of the systematic uncertainties on the amplitude A at Δm_s = 0, 5, 10, 15 and 20 ps^{-1}.

VI. SUMMARY

We search for B_s^0 flavor oscillations using $B_s^0 \to D_s^- \ell^+ X$ decays recorded with the CDF II Detector during the Run II of the Fermilab Tevatron Collider. The D_s^- meson is reconstructed in three decay modes: $\phi\pi^-$, $K^{*0}K^-$ and $\pi^+\pi^-\pi^-$. Opposite side lepton and jet charge tags provide information about the B_s^0 production flavor. Using an amplitude scan method, we obtain

$$\begin{aligned} \Delta m_s &> 6.7 \text{ ps}^{-1} \text{ @ } 95\% \text{ C.L.} \\ \text{expected sensitivity} &= 10.4 \text{ ps}^{-1} \end{aligned}$$

VII. COMBINED $B_S^0 \to D_S^-(3)\pi$ AND $B_S^0 \to D_S^-\ell^+X$ ANALYSES

Two independent analyses of the B_s^0 mixing parameter Δm_s have been done: using $B_s^0 \to D_s^-(3)\pi$ decays [9], and this analysis. In each of them an amplitude scan is performed, to determine the sensitivity to Δm_s and to set a lower limit on Δm_s at a 95% confidence level. For the purpose of combining results, these are treated as independent measurements of a same physics quantity [7]. For each Δm_s value, the corresponding amplitude values measured in the two analyses are averaged as in Equation 9. The combined amplitude scan of the two analyses is shown in Figure 10. The resulting combined Δm_s sensitivity is 13.0 ps^{-1}, and the observed 95% C.L. limit is $\Delta m_s > 8.6$ ps^{-1}.

$$A = \left(\frac{A_1}{\sigma_{A_1}^2} + \frac{A_2}{\sigma_{A_2}^2}\right)\sigma_A^2, \qquad \text{with} \qquad \frac{1}{\sigma_A^2} = \frac{1}{\sigma_{A_1}^2} + \frac{1}{\sigma_{A_2}^2} \tag{9}$$

Acknowledgments

We thank the Fermilab staff and the technical staffs of the participating institutions for their vital contributions. This work was supported by the U.S. Department of Energy and National Science

Foundation; the Italian Istituto Nazionale di Fisica Nucleare; the Ministry of Education, Culture, Sports, Science and Technology of Japan; the Natural Sciences and Engineering Research Council of Canada; the National Science Council of the Republic of China; the Swiss National Science Foundation; the A.P. Sloan Foundation; the Bundesministerium für Bildung und Forschung, Germany; the Korean Science and Engineering Foundation and the Korean Research Foundation; the Particle Physics and Astronomy Research Council and the Royal Society, UK; the Russian Foundation for Basic Research; the Comisión Interministerial de Ciencia y Tecnología, Spain; in part by the European Community's Human Potential Programme under contract HPRN-CT-2002-00292; and the Academy of Finland.

---

[1] S. Eidelman et al. [Particle Data Group], "Review of particle physics", Phys. Lett. B **592**, 1 (2004)
[2] D. Acosta et al. [CDF Collaboration], Phys Rev. D **71**, 032001 (2005)
[3] See *Study of B_s^0 Oscillations Using Semileptonic $B_s^0 \to D_s^- \ell^+ X$ Decays*, available through `http://www-cdf.fnal.gov/physics/new/bottom/bottom.html`
[4] See *Improved Jet Charge Tagging in the Semileptonic Sample*, available through `http://www-cdf.fnal.gov/physics/new/bottom/bottom.html`
[5] See *Likelihood Based Soft Electron Tagging* and *Likelihood Based Soft Muon Tagging*, available through `http://www-cdf.fnal.gov/physics/new/bottom/bottom.html`
[6] See *Scale Factors for Proper Time Uncertainties*, available through `http://www-cdf.fnal.gov/physics/new/bottom/bottom.html`
[7] H.G. Moser et. al., "Mathematical methods for $B^0\bar{B}^0$ oscillations analyses", NIM A384, 491-505 (1997)
[8] See *Measurement of B_d^0 Oscillations and Calibration of Flavor Tagging*, available through `http://www-cdf.fnal.gov/physics/new/bottom/bottom.html`
[9] See *Updated Study of B_s^0 Oscillations in $B_s^0 \to D_s^-(3)\pi$*, available through `http://www-cdf.fnal.gov/physics/new/bottom/bottom.html`

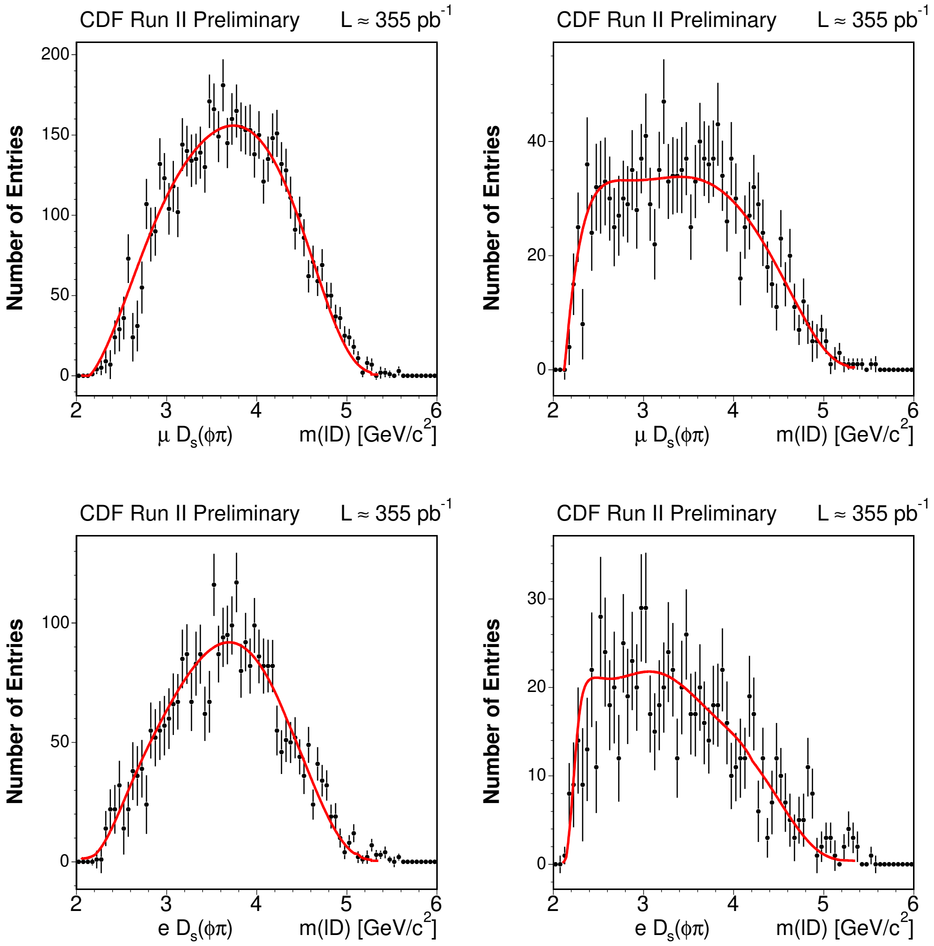

FIG. 1: The $m_{\ell^+ D_s^-}$ invariant mass distributions of $D_s^- \to \phi\pi^-$ candidates. Clockwise: muon SVT, muon non-SVT, electron SVT and electron non-SVT.

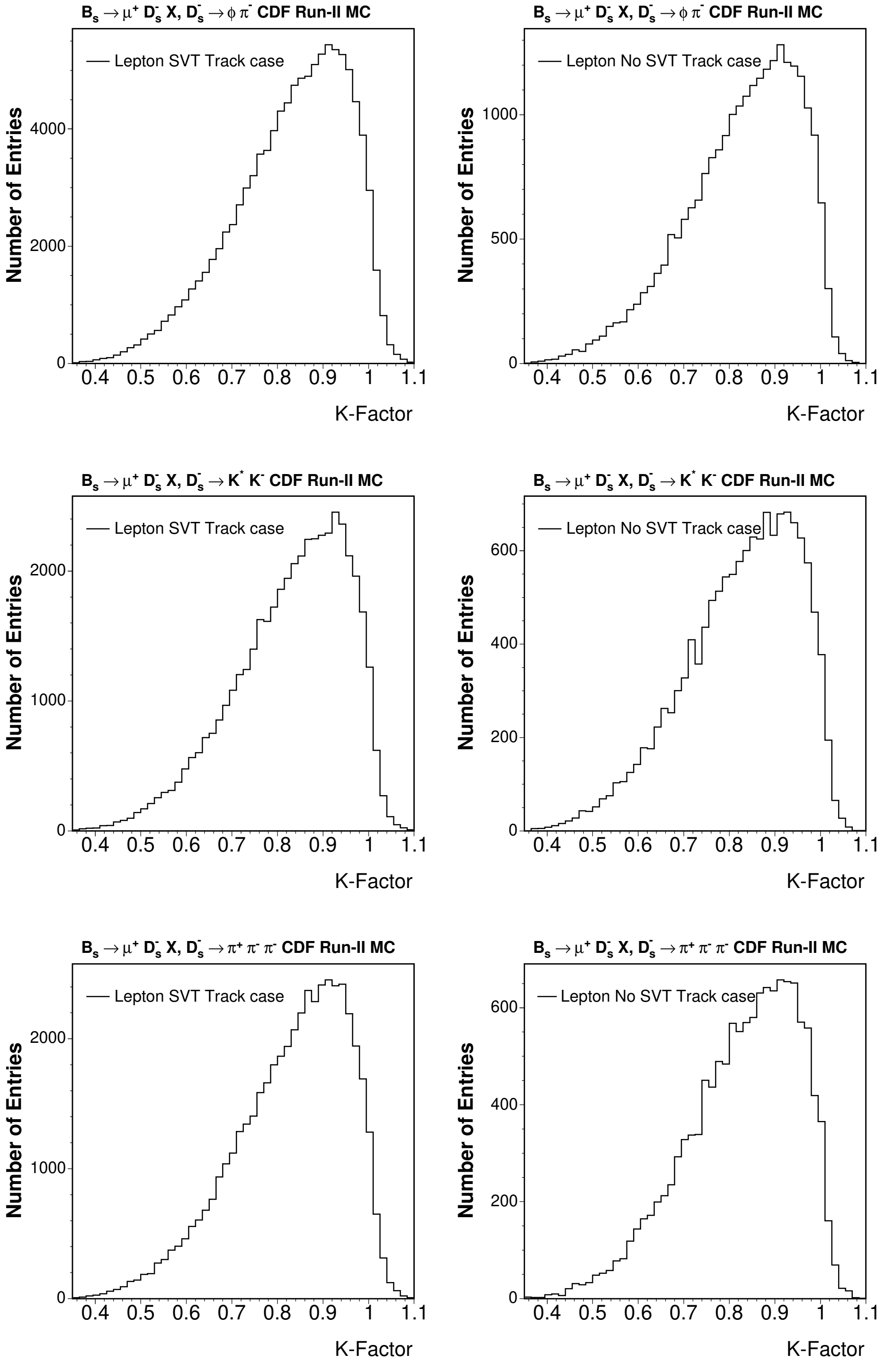

FIG. 2: Overall k-factor distributions, from top to bottom: $D_s^- \to \phi\pi^-$, $D_s^- \to K^{*0}K^-$ and $D_s^- \to \pi^+\pi^-\pi^-$. Left (right) column corresponds to muon SVT (muon non-SVT).

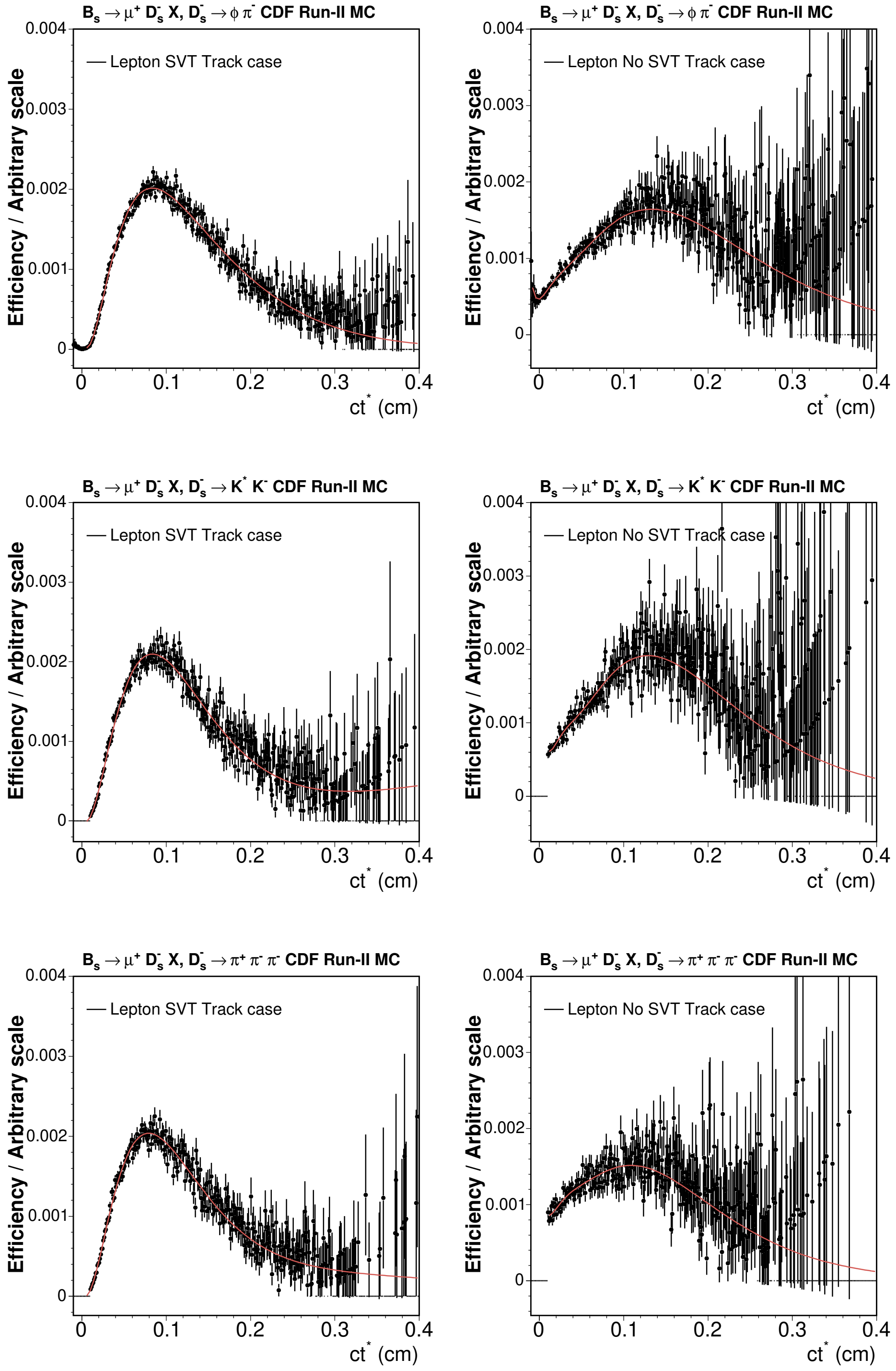

FIG. 3: Some ct^*-efficiency curves, from top to bottom: $D_s^- \to \phi\pi^-$, $D_s^- \to K^{*0}K^-$ and $D_s^- \to \pi^+\pi^-\pi^-$. Left (right) column corresponds to muon SVT (muon non-SVT).

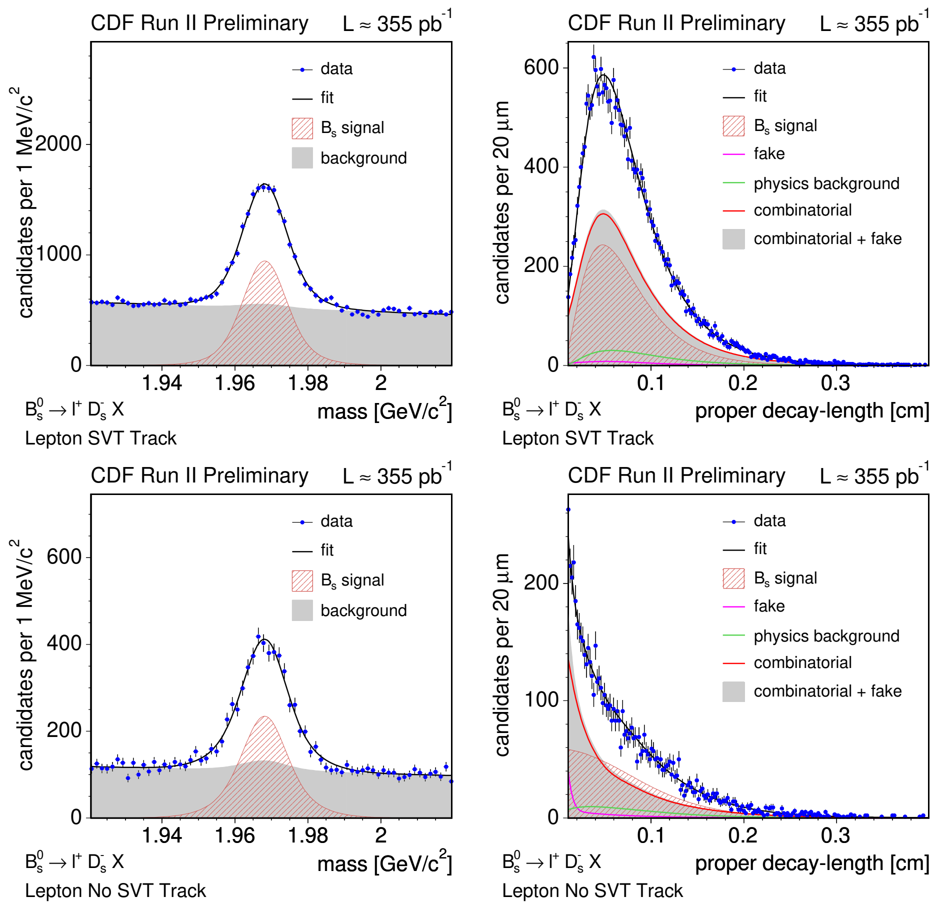

FIG. 4: The D_s^- mass (left) and ct^* (right) fit projections of all $B_s^0 \to D_s^- \ell^+ X$ decays. From top to bottom: lepton SVT and lepton non-SVT.

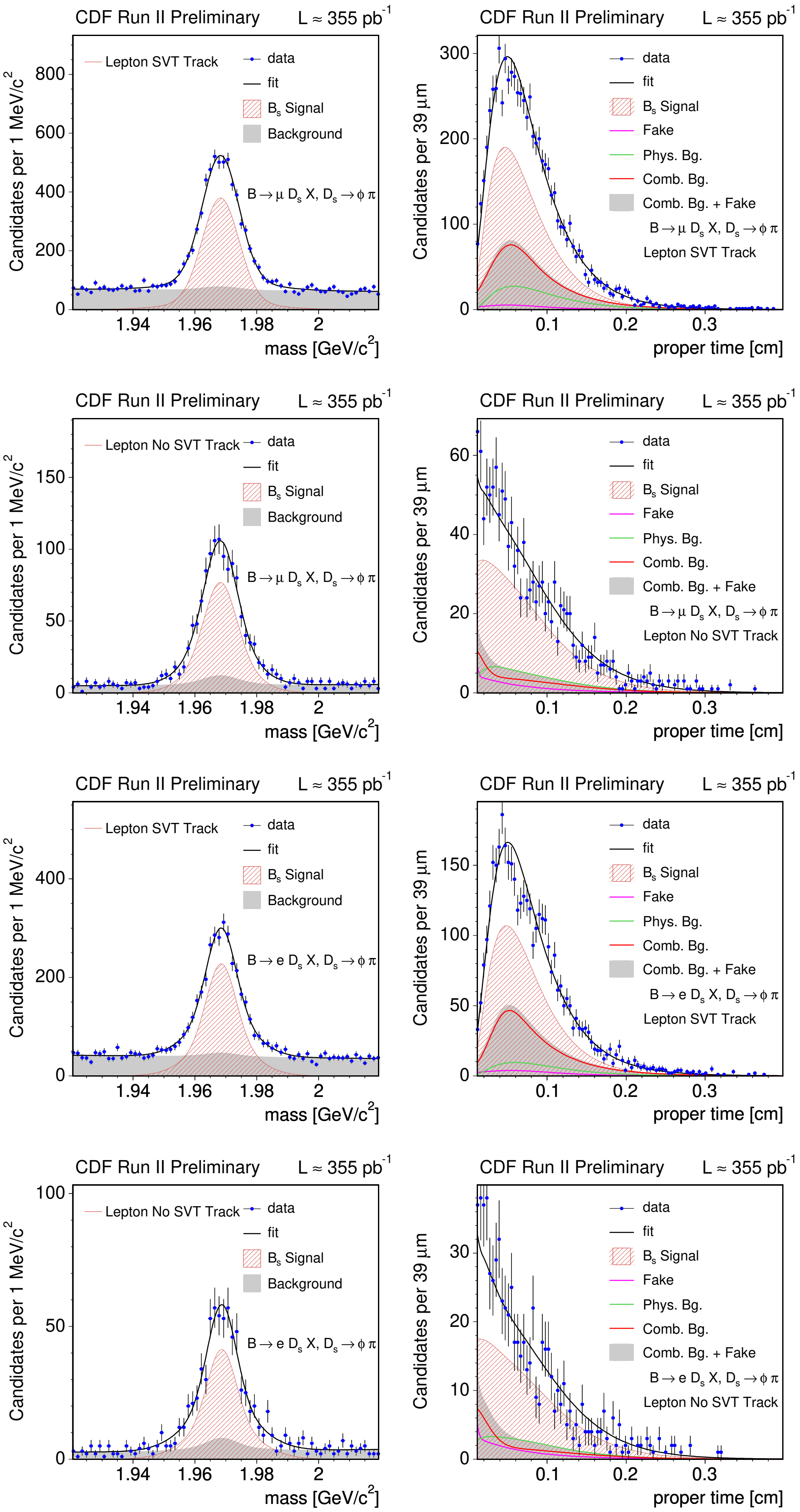

FIG. 5: The D_s^- mass (left) and ct^* (right) fit projections of $D_s^- \to \phi\pi^-$ decays. From top to bottom: muon SVT, muon non-SVT, electron SVT and electron non-SVT.

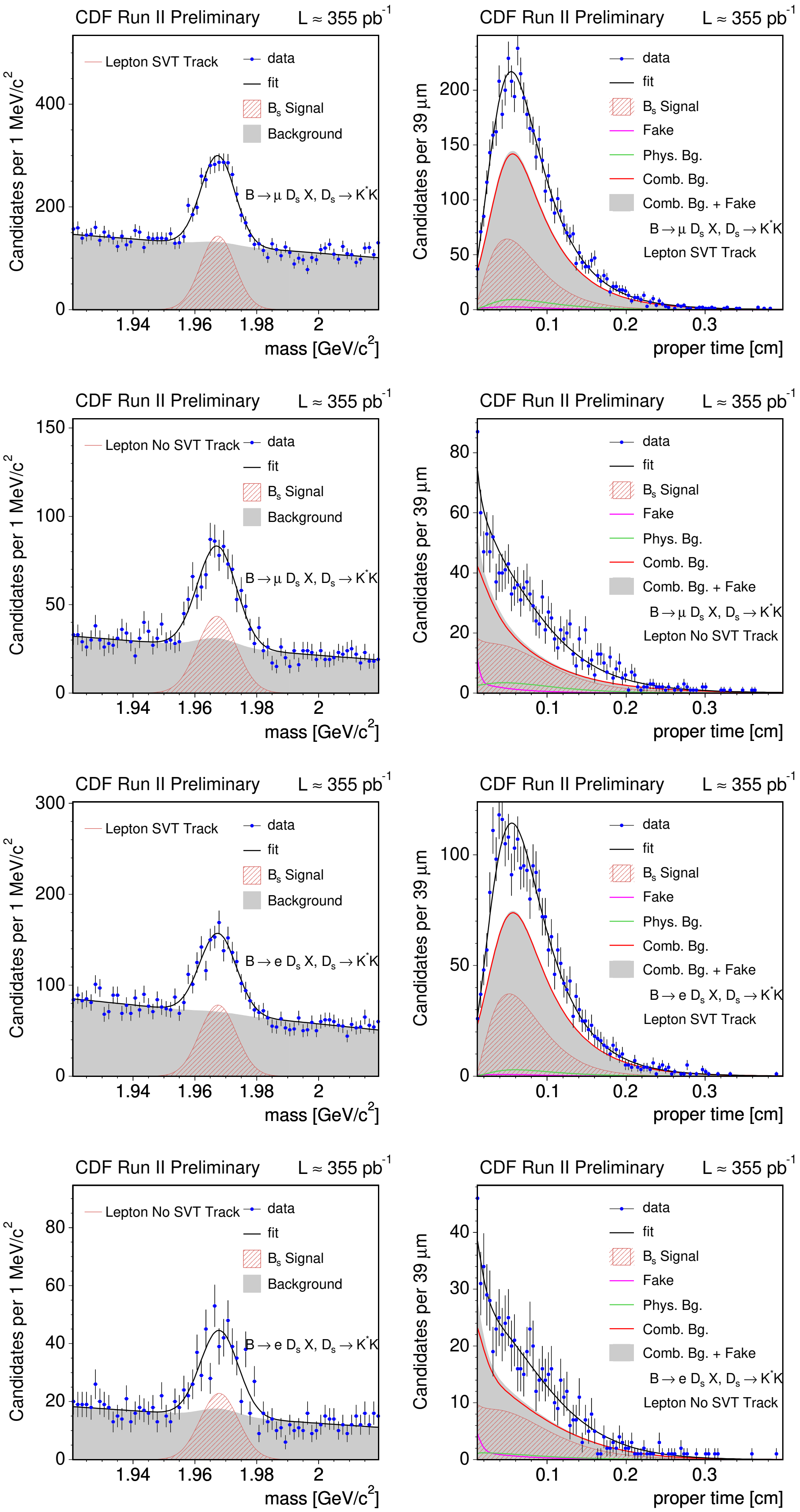

FIG. 6: The D_s^- mass (left) and ct^* (right) fit projections of $D_s^- \to K^{*0}K^-$ decays. From top to bottom: muon SVT, muon non-SVT, electron SVT and electron non-SVT.

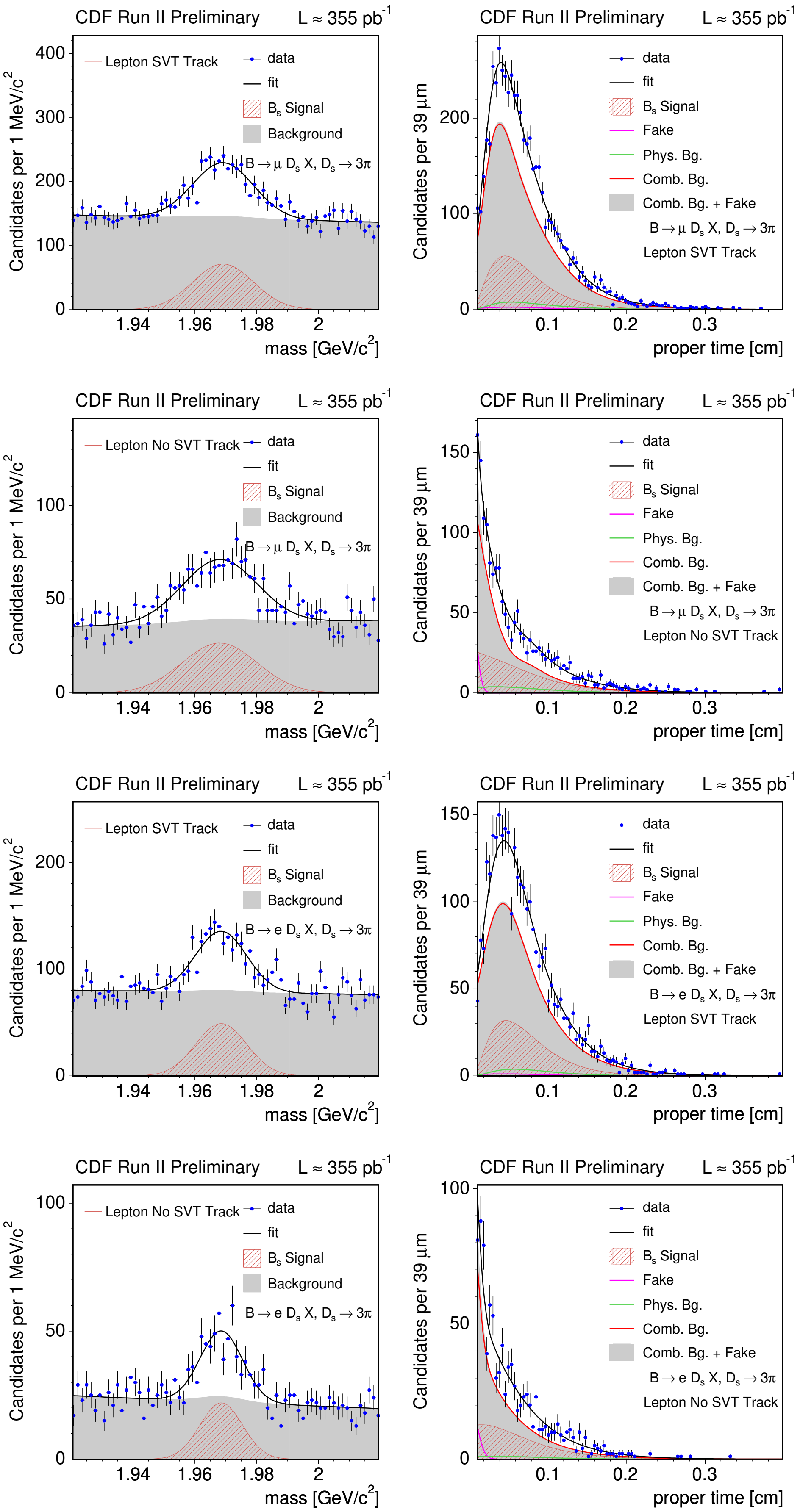

FIG. 7: The D_s^- mass (left) and ct^* (right) fit projections of $D_s^- \to \pi^+\pi^-\pi^-$ decays. From top to bottom: muon SVT, muon non-SVT, electron SVT and electron non-SVT.

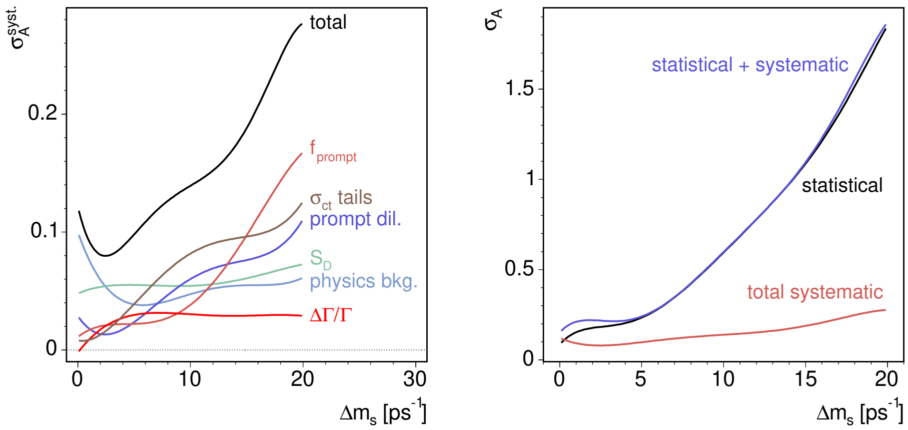

FIG. 8: Parameterization of the overall systematic uncertainty as a function of Δm_s (left), and comparison of the overall systematic and the statistical uncertainties (right).

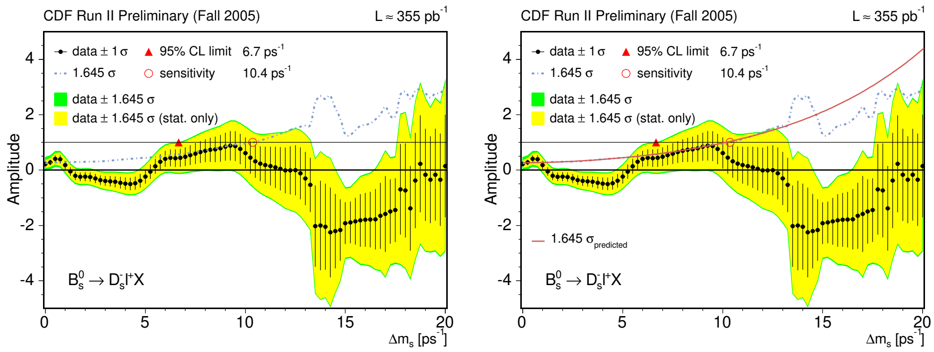

FIG. 9: Amplitude scan for $B_s^0 \to D_s^- \ell^+ X$ decays (left) with the predicted significance overlaid (right).

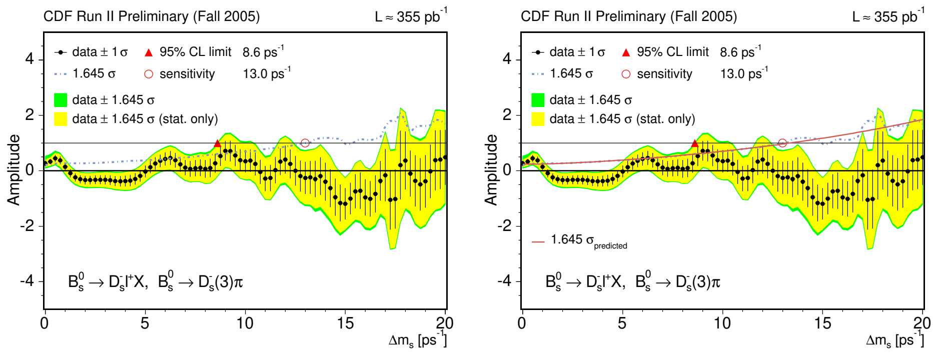

FIG. 10: Combined amplitude scan for $B_s^0 \to D_s^-(3)\pi$ and $B_s^0 \to D_s^- \ell^+ X$ decays (left) with the predicted significance overlaid (right).